Supplement of Atmos. Chem. Phys., 22, 2909–2935, 2022
https://doi.org/10.5194/acp-22-2909-2022-supplement

Atmospheric Chemistry and Physics
Open Access

Supplement of

Relative importance of high-latitude local and long-range-transported dust for Arctic ice-nucleating particles and impacts on Arctic mixed-phase clouds

Yang Shi et al.

Correspondence to: Xiaohong Liu (xiaohong.liu@tamu.edu)

Text S1: K14 dust emission parameterization

Kok et al. (2014a, b) (K14) is a physically based dust emission scheme that removes the need to use an empirical dust soil erodibility map in other parameterizations (e.g., Zender et al., 2003). The vertical dust emission flux, F_d (kg m^{-2} s^{-1}), is given by

$$F_d = C_d f_{bare} f_{clay} \frac{\rho_a(u_*^2-u_{*t}^2)}{u_{*st}} \left(\frac{u_*}{u_{*t}}\right)^{C_\alpha \frac{u_{*st}-u_{*st0}}{u_{*st0}}}, (u_* > u_{*t}), \quad \text{(S1)}$$

where C_d is the dimensionless dust emission coefficient, f_{bare} is the fraction of the surface consisting of bare soil, f_{clay} is the soil clay fraction, ρ_a (kg m^{-3}) is the air density, u_* (m s^{-1}) is the soil friction velocity, u_{*t} (m s^{-1}) is the threshold of soil friction velocity above which saltation occurs, u_{*st} (m s^{-1}) is the soil threshold friction velocity standardized to standard atmospheric density, u_{*st0} (m s^{-1}) is the standardized threshold friction velocity of an optimally erodible soil, and C_α is the dimensionless constant scaling the fragmentation exponent (α).

Text S2: Ice nucleation parameterizations

In this section, we introduced five ice nucleation parameterizations used in this study. They can be classified into two types: the stochastic approach, which treats ice nucleation as a time-dependent process, and the deterministic approach, which assumes that ice nucleation is time-invariant and only depends on temperature and aerosol properties. In this study, the CNT parameterization follows the stochastic approach, while the other four parameterizations follow the deterministic approach.

S2.1 CNT parameterization

The classical nucleation theory (CNT) scheme is used for heterogeneous ice nucleation in mixed-phase clouds in EAMv1 simulations. This parameterization was first implemented in a global climate model by Hoose et al. (2010), and further improved by Wang et al. (2014) by introducing a probability density function of contact angles (α-PDF) for immersion freezing of natural dust. In CNT, immersion/condensation, contact, and deposition nucleation on dust and BC are treated. The rate of heterogeneous nucleation per aerosol particle and time, J_{het}, is expressed by

$$J_{het} = \frac{A' r_N^2}{\sqrt{f}} \exp\left(\frac{-\Delta g^{\#} - f \Delta g_g^o}{kT}\right), \tag{S2}$$

where A' is a prefactor, r_N is the aerosol particle radius, f is a form factor describing the aerosol's ice nucleating ability, $\Delta g^{\#}$ is the activation energy, Δg_g^o is the homogeneous energy of germ formation, k is the Boltzmann constant, and T is the temperature in K. The factor, f, is a function of contact angle, α, in the form,

$$f = \frac{1}{4}(2+m)(1-m)^2, \tag{S3}$$

where $m \equiv cos\alpha$. The contact angle is assumed to follow a log-normal distribution in the form,

$$p(\alpha) = \frac{1}{\alpha\sigma\sqrt{2\pi}} \exp\left(-\frac{(\ln(\alpha) - \ln(\mu))^2}{2\sigma^2}\right), \tag{S4}$$

where μ is the mean contact angle and σ is the standard deviation.

We do not consider the differences in the mineralogical composition in different dust sources. Thus, dust particles originated from different sources are treated the same in the CNT (i.e., same contact angle distribution). The parameterization considers the immersion freezing point depression by coating of sulfate aerosols (Hoose et al., 2010). However, this effect has no differences for HLD and LLD, because aerosol species (e.g, dust, sulfate) are assumed to be internally mixed within an aerosol mode in the MAM4 aerosol module (Liu et al., 2016).

S2.2 D15 parameterization

The DeMott et al. (2015; D15) parameterization is a dust immersion freezing ice nucleation parameterization derived from a combination of laboratory and field data. The laboratory data are from ice nucleation experiments on Saharan and Asian desert dust using the Aerosol Interaction and Dynamics in the Atmosphere chamber. The field data were collected over the Pacific Ocean basin and US Virgin Islands, which are dominated by Asian and Saharan desert dust, respectively. Thereby, D15 can be regarded as a LLD ice nucleation parameterization in our study, though it is also applied to HLD in Figure 8e for sensitivity studies. In D15, dust INP number concentration, n_{INP} (std L^{-1}), is related to temperature, T_k (K), and the number concentration of dust particles larger than 0.5 μm, $n_{a>0.5\mu m}$ (std cm^{-3}), in the form,

$$n_{INP}(T_k) = (cf)(n_{a>0.5\mu m})^{\alpha(273.16-T_k)+\beta} \exp\left(\gamma(273.16 - T_k) + \delta\right), \qquad \text{(S5)}$$

where cf = 3, α = 0, β = 1.25, γ = 0.46, and δ = -11.6.

S2.3 SM20 parameterization

The Sanchez-Marroquin et al. (2020; SM20) parameterization is based on aircraft-collected freshly emitted Icelandic dust samples and thus is treated as a parameterization for HLD in our study. It is an immersion freezing ice nucleation scheme formulated in terms of the ice-nucleating active surface site density (INAS). The total INP concentration, n_{INP} (L^{-1}), is given by

$$n_{INP} = n_{HLD}\{1 - \exp\left[-S_{ae} n_s\right]\}, \qquad \text{(S6)}$$

where n_{HLD} (L^{-1}) is the number concentration of HLD, S_{ae} (m^2) is the surface area of a single HLD particle, and n_s (m^{-2}) is the density of active sites. n_s is in the form

$$n_s(T) = 10^{-0.0337-0.199T}, \qquad \text{(S7)}$$

where T is temperature in ^{o}C.

S2.4 Sc20 parameterization

The Schill et al. (2020; Sc20) parameterization is an INAS-based immersion freezing ice nucleation parameterization based on smoke from western US wildfires and grassland prescribed burns. It is an ice nucleation parameterization for biomass burning black carbon (BC), but we apply it to BC from both biomass burning and fossil fuel combustion. The total INP concentration is given by the same equation as Eq.(S6), except n_{HLD} is replaced by n_{BC}, which is the number concentration of BC. The n_s fit for Sc20 is given by

$$n_s(T) = \exp(1.844 - 0.684T - 0.00597T^2), \tag{S8}$$

where T is temperature in °C.

S2.5 M18 parameterization

The McCluskey et al. (2018; M18) parameterization is an INAS based immersion freezing ice nucleation parameterization for sea spray aerosols (SSAs; includes sea salt and marine organic aerosol) derived from pristine marine air mass measurements at the Mace Head Research Station. The total INP concentration is given by the same equation as Eq.(S6), except n_{HLD} is replaced by n_{SSA}, which is the number concentration of SSA. The n_s fit for M18 is given by

$$n_s(T_k) = \exp\left(-0.545(T_k - 273.15) + 1.0125\right), \tag{S9}$$

where T_k is temperature in K.

S2.6 Discussion regarding the choice of dust ice nucleation parameterizations

In this study, we use three dust ice nucleation parameterizations (i.e., CNT, D15, and SM20). CNT is chosen because it is the default ice nucleation scheme for EAMv1. We use D15 because it is found to produce the most reasonable INP concentrations in EAMv1 based on our earlier study (Shi and Liu, 2019). There are various other LLD INP parameterizations, many of which are INAS-based (e.g., Niemand et al., 2012; Ullrich et al., 2017). The Niemand et al. (2012) parameterization was tested in Shi and Liu (2019) and was found to overestimate the Arctic INP concentrations with corrected dust concentrations in EAMv1. There are also INP parameterizations based on dust minerology (e.g., Atkinson et al., 2013; Harrison et al., 2019), which are not used because we do not represent dust speciation in the current model. There are not a lot of HLD INP parameterizations (or even data) as compared to LLD INP schemes. To our knowledge, Paramonov et al. (2018) analyze the ice nucleation ability of soil samples collected from Iceland and provide an INAS-based fit. We use SM20 which was developed based on airborne samples rather than Paramonov et al. (2018) in our study, due to the possible large differences between soil samples and airborne dust samples.

Reference

Atkinson, J. D., Murray, B. J., Woodhouse, M. T., Whale, T. F., Baustian, K. J., Carslaw, K. S., Dobbie, S., O'Sullivan, D., and Malkin, T. L.: The importance of feldspar for ice nucleation by mineral dust in mixed-phase clouds, Nature, 498, 355–358, https://doi.org/10.1038/nature12278, 2013.

DeMott, P. J., Prenni, A. J., McMeeking, G. R., Sullivan, R. C., Petters, M. D., Tobo, Y., Niemand, M., Möhler, O., Snider, J. R., Wang, Z., and Kreidenweis, S. M.: Integrating laboratory and field data to quantify the immersion freezing ice nucleation activity of mineral dust particles, Atmos. Chem. Phys., 15, 393–409, https://doi.org/10.5194/acp-15-393-2015, 2015.

Harrison, A. D., Lever, K., Sanchez-Marroquin, A., Holden, M. A., Whale, T. F., Tarn, M. D., McQuaid, J. B., and Murray, B. J.: The ice-nucleating ability of quartz immersed in water and its atmospheric importance compared to K-feldspar, 19, 2019.

Hoose, C., Kristjánsson, J. E., Chen, J.-P., and Hazra, A.: A Classical-Theory-Based Parameterization of Heterogeneous Ice Nucleation by Mineral Dust, Soot, and Biological Particles in a Global Climate Model, 67, 2483–2503, https://doi.org/10.1175/2010JAS3425.1, 2010.

Kok, J. F., Mahowald, N. M., Fratini, G., Gillies, J. A., Ishizuka, M., Leys, J. F., Mikami, M., Park, M.-S., Park, S.-U., Van Pelt, R. S., and Zobeck, T. M.: An improved dust emission model – Part 1: Model description and comparison against measurements, Atmos. Chem. Phys., 14, 13023–13041, https://doi.org/10.5194/acp-14-13023-2014, 2014a.

Kok, J. F., Albani, S., Mahowald, N. M., and Ward, D. S.: An improved dust emission model – Part 2: Evaluation in the Community Earth System Model, with implications for the use of dust source functions, Atmos. Chem. Phys., 14, 13043–13061, https://doi.org/10.5194/acp-14-13043-2014, 2014b.

Liu, X., Ma, P.-L., Wang, H., Tilmes, S., Singh, B., Easter, R. C., Ghan, S. J., and Rasch, P. J.: Description and evaluation of a new four-mode version of the Modal Aerosol Module (MAM4) within version 5.3 of the Community Atmosphere Model, Geosci. Model Dev., 9, 505–522, https://doi.org/10.5194/gmd-9-505-2016, 2016.

McCluskey, C. S., Ovadnevaite, J., Rinaldi, M., Atkinson, J., Belosi, F., Ceburnis, D., Marullo, S., Hill, T. C. J., Lohmann, U., Kanji, Z. A., O'Dowd, C., Kreidenweis, S. M., and DeMott, P. J.: Marine and Terrestrial Organic Ice-Nucleating Particles in Pristine Marine to Continentally Influenced Northeast Atlantic Air Masses, J. Geophys. Res. Atmos., 123, 6196–6212, https://doi.org/10.1029/2017JD028033, 2018.

Niemand, M., Möhler, O., Vogel, B., Vogel, H., Hoose, C., Connolly, P., Klein, H., Bingemer, H., DeMott, P., Skrotzki, J., and Leisner, T.: A Particle-Surface-Area-Based Parameterization of Immersion Freezing on Desert Dust Particles, 69, 3077–3092, https://doi.org/10.1175/JAS-D-11-0249.1, 2012.

Sanchez-Marroquin, A., Arnalds, O., Baustian-Dorsi, K. J., Browse, J., Dagsson-Waldhauserova, P., Harrison, A. D., Maters, E. C., Pringle, K. J., Vergara-Temprado, J., Burke, I. T., McQuaid, J. B., Carslaw, K. S., and Murray, B. J.: Iceland is an episodic source of atmospheric ice-nucleating particles relevant for mixed-phase clouds, Sci. Adv., 6, eaba8137, https://doi.org/10.1126/sciadv.aba8137, 2020.

Schill, G. P., DeMott, P. J., Emerson, E. W., Rauker, A. M. C., Kodros, J. K., Suski, K. J., Hill, T. C. J., Levin, E. J. T., Pierce, J. R., Farmer, D. K., and Kreidenweis, S. M.: The contribution of black carbon to global ice nucleating particle concentrations relevant to mixed-phase clouds, Proc Natl Acad Sci USA, 117, 22705–22711, https://doi.org/10.1073/pnas.2001674117, 2020.

Shi, Y. and Liu, X.: Dust Radiative Effects on Climate by Glaciating Mixed-Phase Clouds, Geophys. Res. Lett., 46, 6128–6137, https://doi.org/10.1029/2019GL082504, 2019.

Ullrich, R., Hoose, C., Möhler, O., Niemand, M., Wagner, R., Höhler, K., Hiranuma, N., Saathoff, H., and Leisner, T.: A New Ice Nucleation Active Site Parameterization for Desert Dust and Soot, 74, 699–717, https://doi.org/10.1175/JAS-D-16-0074.1, 2017.

Wang, Y., Liu, X., Hoose, C., and Wang, B.: Different contact angle distributions for heterogeneous ice nucleation in the Community Atmospheric Model version 5, Atmos. Chem. Phys., 14, 10411–10430, https://doi.org/10.5194/acp-14-10411-2014, 2014.

Table S1. Arctic burden efficiency (10^{-3} mg m^{-2}) (mg m^{-2} s^{-1})$^{-1}$.

	Annual	MAM	JJA	SON	DJF
Arc	15.88	20.96	20.82	10.49	15.10
NAm	1.99	2.78	3.78	1.68	0.84
NAf	0.62	1.11	0.50	0.35	0.32
CAs	2.58	2.66	4.11	2.51	1.01
MSA	0.76	1.50	0.45	0.49	0.63
EAs	2.42	2.19	2.99	2.02	2.75
RoW	0.00	0.00	0.00	0.00	0.01

Table S2. Yearly (2007 to 2011) averaged HLD emission flux (Tg yr^{-1}) in CTRL and HLD_half.

	CTRL	HLD_half
2007	129.2	64.2
2008	213.8	103.4
2009	114.2	50.8
2010	127.1	53.2
2011	137.8	56.7

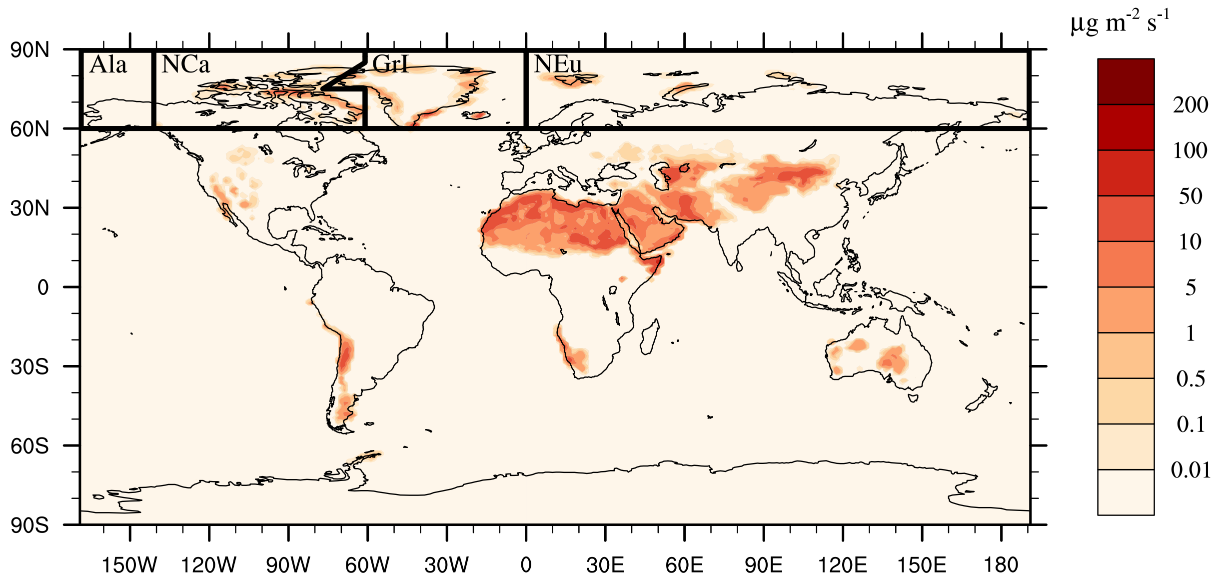

Figure S1. Same as Figure 1a, but with four sub-sources tagged in the Arctic (Ala: Alaska, NCa: North Canada; GrI: Greenland and Iceland; NEu: North Eurasia).

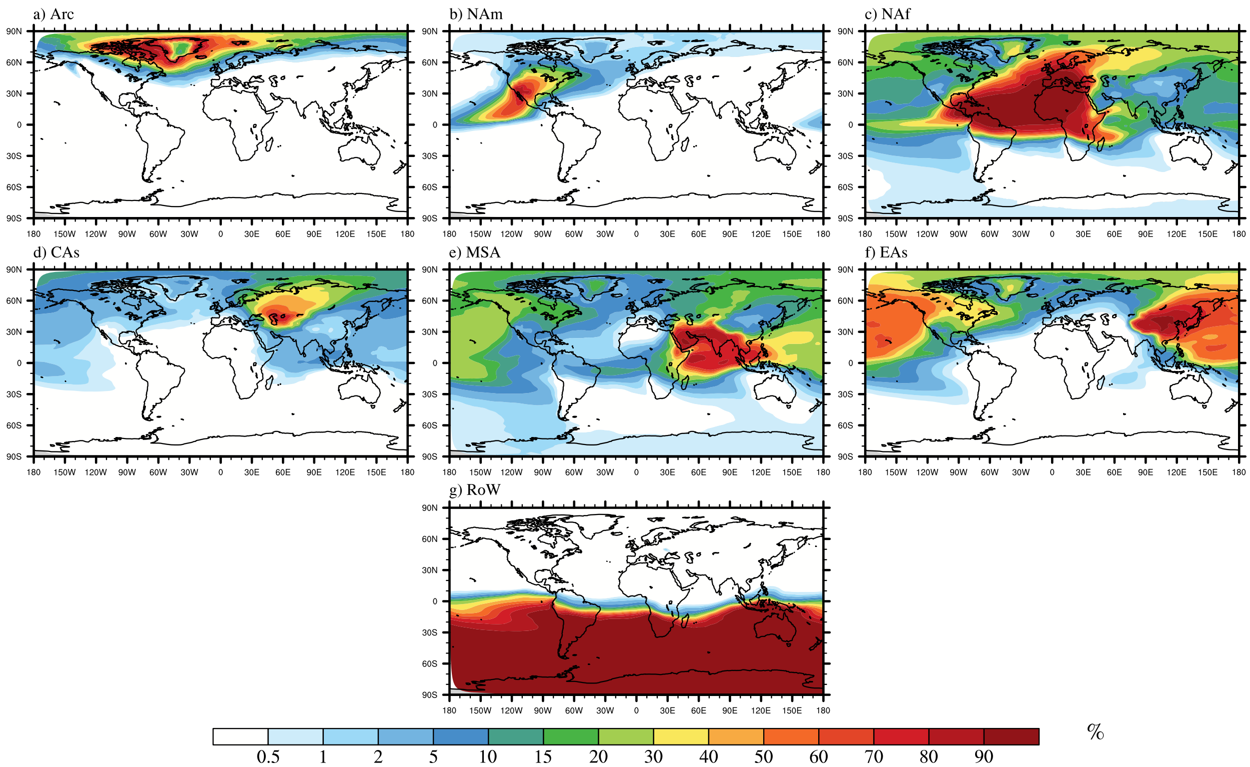

Figure S2. Global distribution of relative contributions (%) to the annual mean (2007 to 2011) dust column burden from each tagged source region.

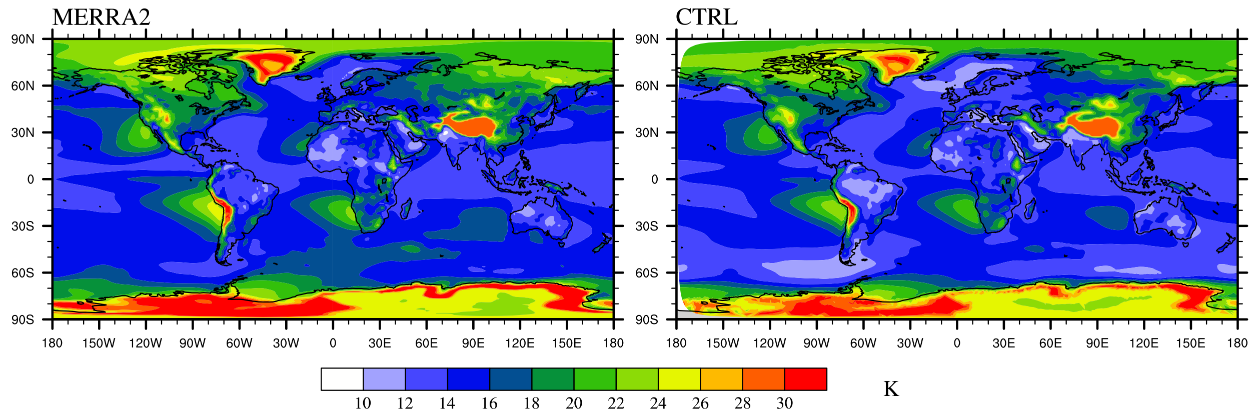

Figure S3. Annual mean (2007 to 2011) lower tropospheric stability (LTS) from MERRA2 reanalysis data and the CTRL simulation. LTS is defined as the potential temperature difference between 700 and 1000 hPa. The LTS from the CTRL simulation agrees well with the MERRA2 data.

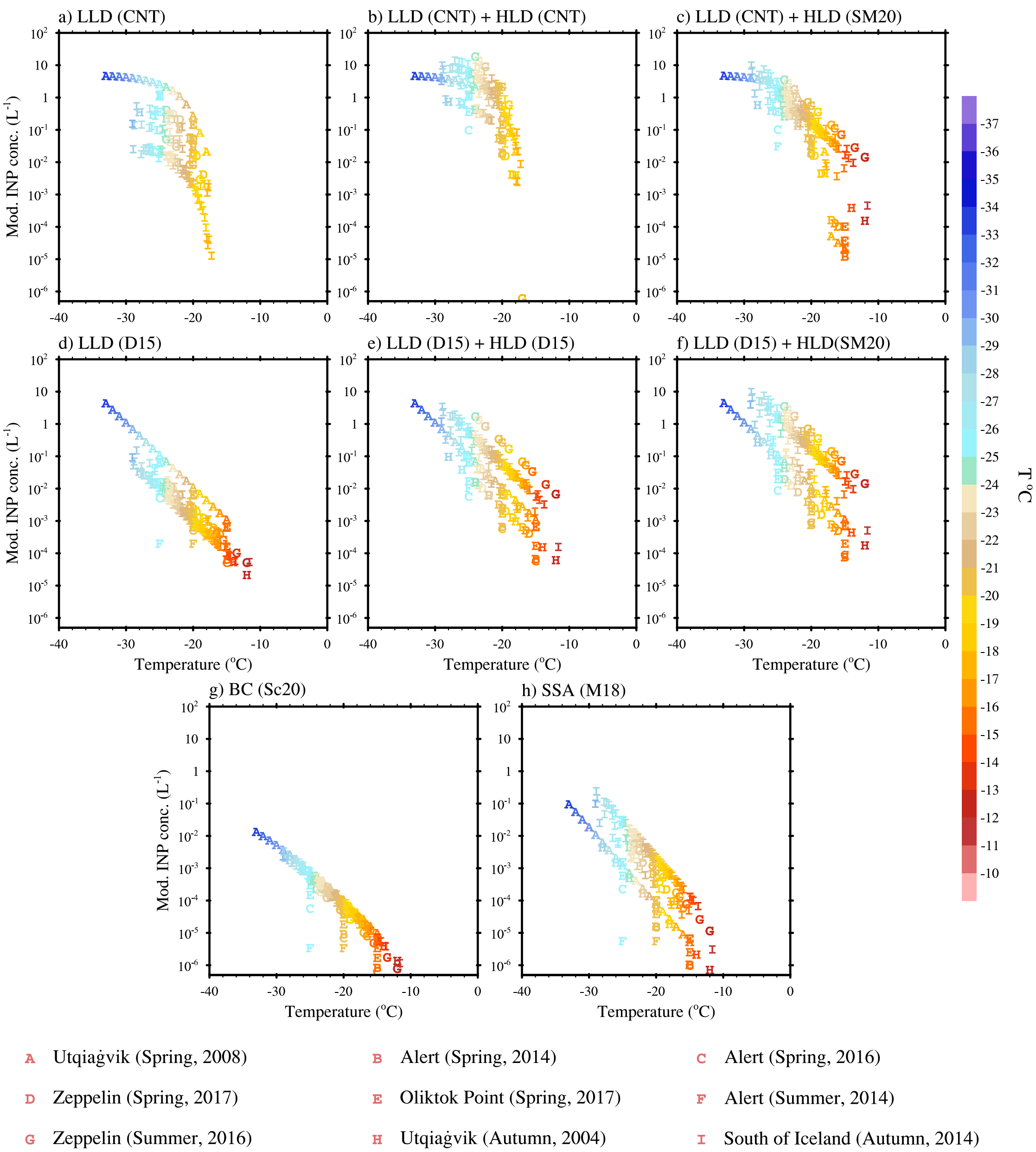

Figure S4. Simulated INP concentrations as a function of temperature. The simulated INP concentrations are derived from a) LLD using classical nucleation theory (CNT), b) LLD and HLD, both using CNT, c) LLD using CNT and HLD using Sanchez-Marroquin et al (2020; SM20), d) LLD using DeMott et al. (2015; D15), e) LLD and HLD, both using D15, f) LLD using D15 and HLD using SM20, g) BC using Schill et al. (2020; Sc20), and h) SSA using McCluskey et al. (2018; M18). The temperature of each data point is also shown by its color. Nine INP datasets are classified by symbols A to I. This figure is based on the same simulated INP concentrations that used from Figure 8.

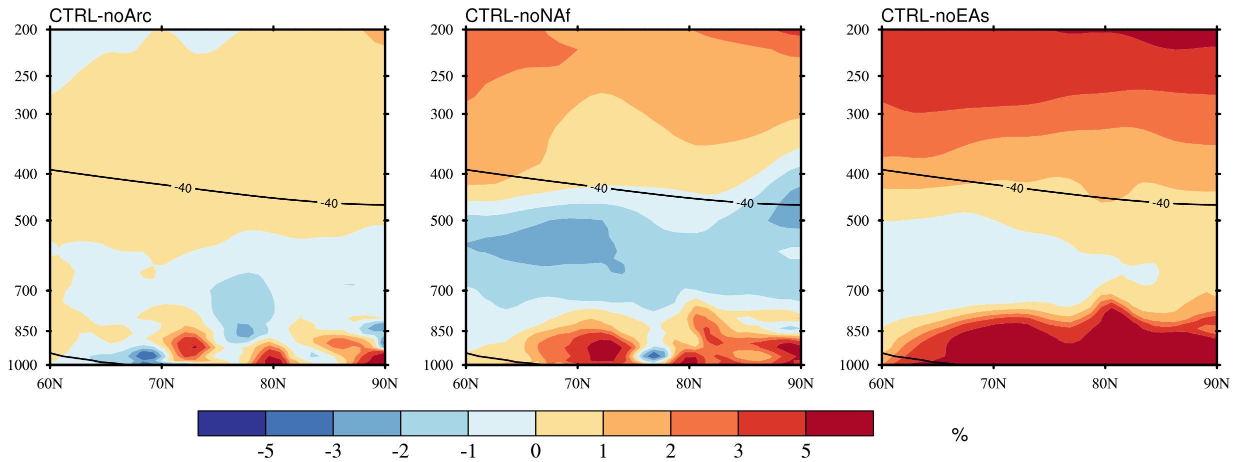

Figure S5. Percentage difference of zonally averaged dust concentration between CTRL and sensitivity experiments (i.e., noArc, noNAf, noEAs). Black contours are zonally averaged temperatures in ^{o}C.

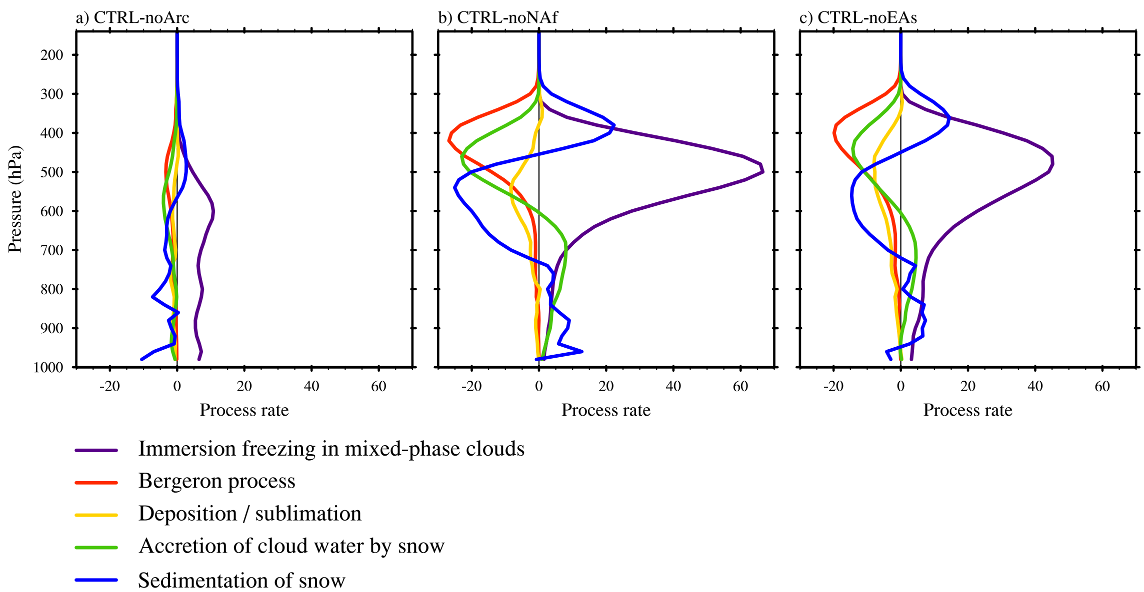

Figure S6. Process budget analysis associated with total ice water tendencies from cloud microphysical processes in the Arctic (unit: 10^{-3} μg kg^{-1} s^{-1}). Only the processes that have large changes are shown in this figure.

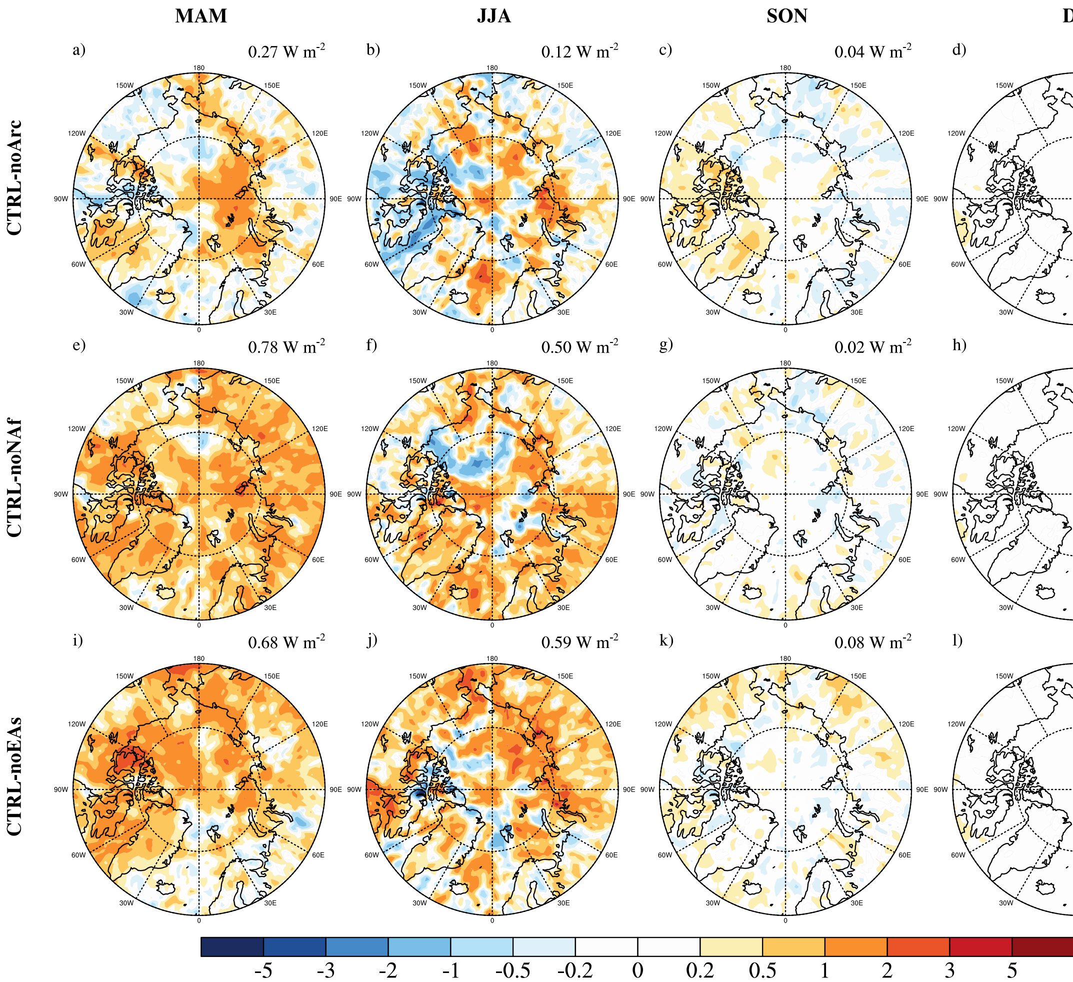

Figure S7. Seasonal changes in shortwave downwelling radiative flux at the surface (unit: W m^{-2}) caused by dust INPs from Arctic (top panel), North Africa (middle panel), and East Asia (bottom panel). The numbers are averaged radiative flux differences in the Arctic.

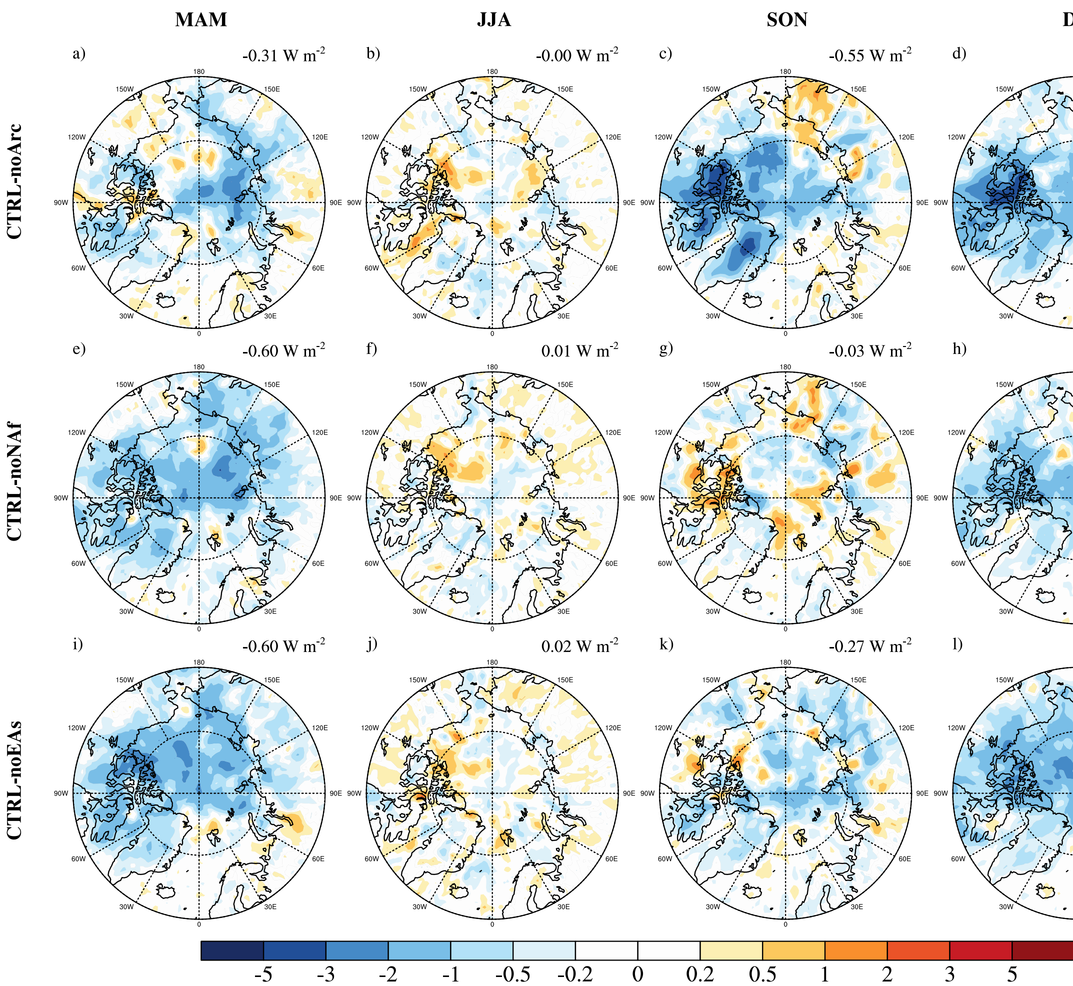

Figure S8. Same as Figure S7, but for longwave downwelling radiative flux.

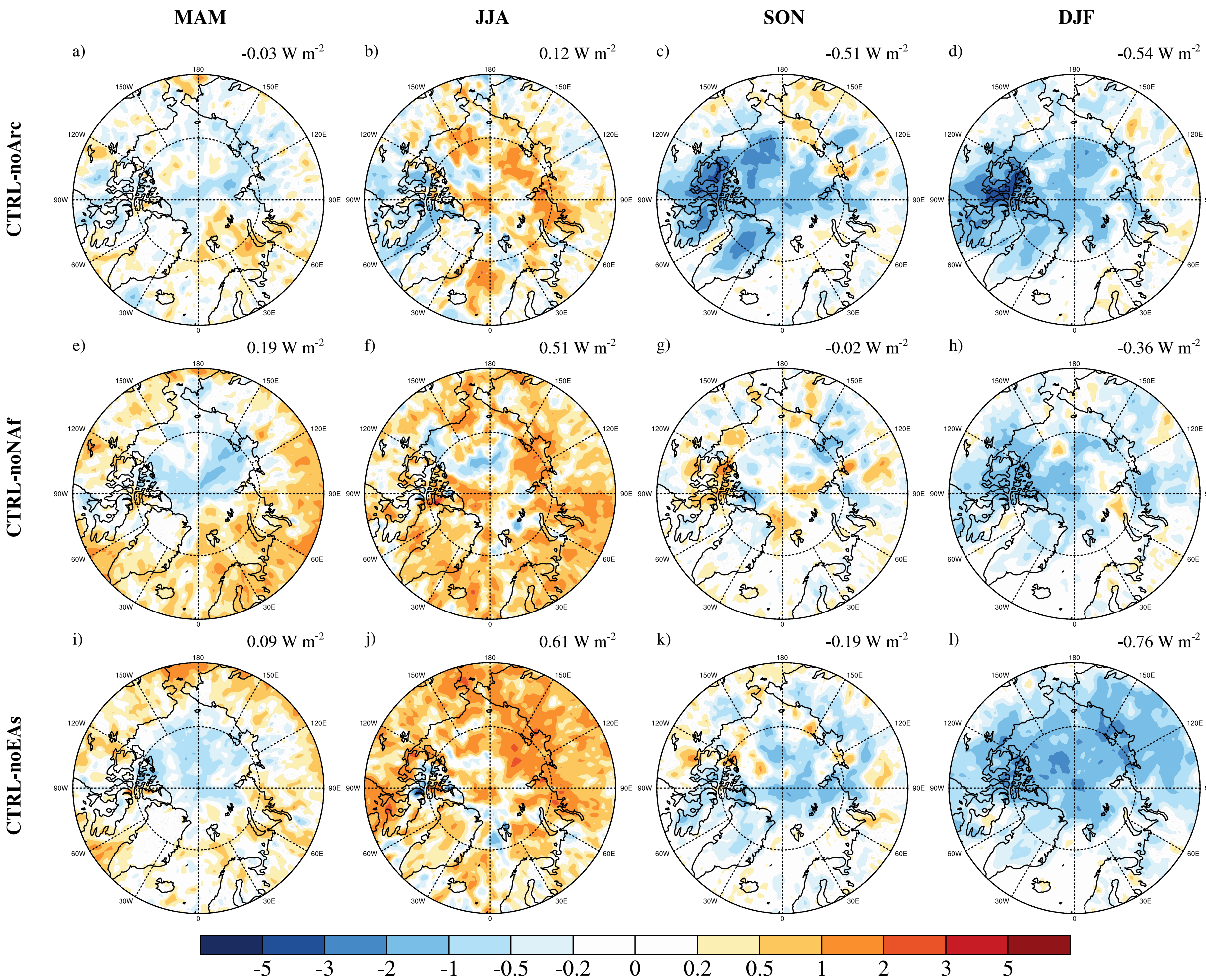

Figure S9. Same as S7, but for net downwelling radiative flux.

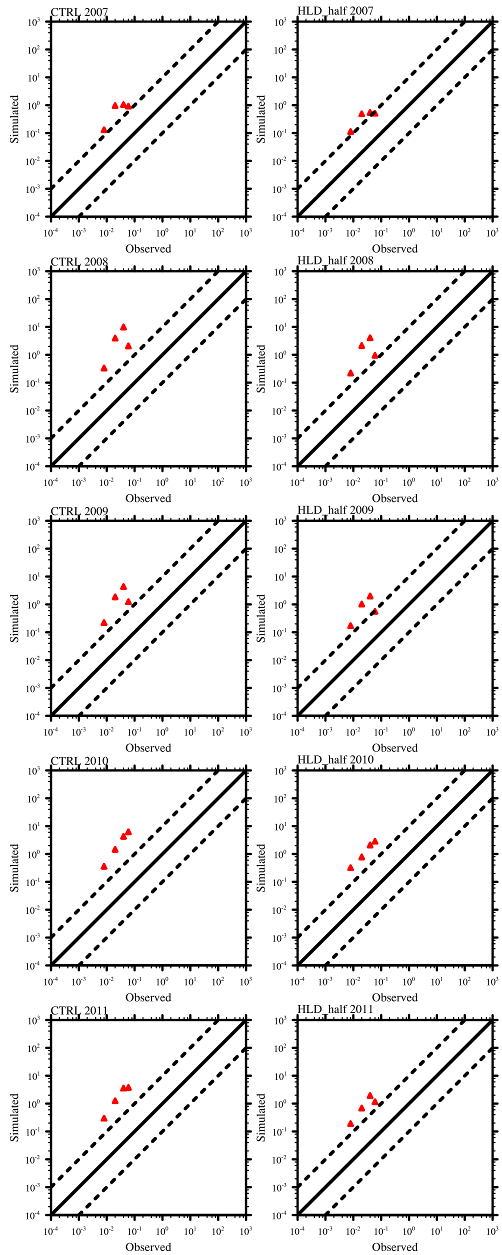

Figure S10. Yearly (2007 to 2011) comparisons of dust deposition fluxes in the Arctic (Greenland) for CTRL and HLD_half. The locations of the markers are shown by the red triangles on Figure 2d. Unit: g m^{-2} yr^{-1}.

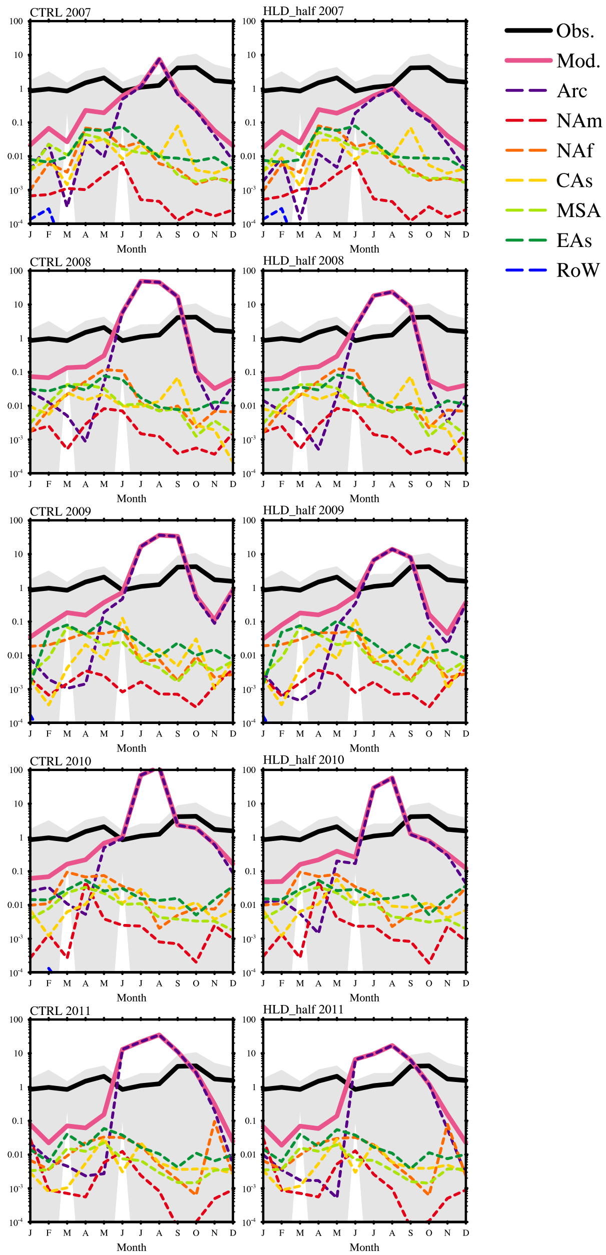

Figure S11. Yearly (2007 to 2011) comparisons of surface dust concentrations at Alert station for CTRL and HLD_half. Unit: μg m^{-3}. The measurements are shown by black solid line, with gray shade representing standard deviation. The simulated total dust concentrations are shown by pink soild line, while contributions from seven tagged sources are shown by colored dashed lines.